Reply

CECILIA JOHANSSON, ANN-SOFI SMEDMAN, AND ULF HÖGSTRÖM

Department of Earth Sciences, Meteorology, Uppsala University, Uppsala, Sweden

JAMES G. BRASSEUR

Department of Mechanical Engineering, The Pennsylvania State University, University Park, Pennsylvania

2 November 2001 and 1 March 2002

1. Introduction

In the comments by E. L Andreas and B. B. Hicks (2002, hereafter AH02), two issues concerning spurious correlation are raised: 1) the reason for the difference in scatter in conventional plots of normalized wind gradient compared to plots of normalized temperature gradient; and 2) the validity of the relationship that was derived in Johansson et al. (2001) for the horizontal velocity variance and the general concept of similarity theory, whereby scales that characterize turbulence structure normalize appropriate moments.

Both issues deal with results obtained when applying Monin–Obukhov (MO) theory. In MO theory the physically relevant characteristic scales in the surface layer are assumed to be derivable from the surface heat flux H_0, the height above the ground z, the buoyancy parameter g/T_0, and the surface stress τ_0. From these, the characteristic velocity scale (the friction velocity u_*) and the characteristic temperature scale (T_*) are

$$u_* = \sqrt{-(\overline{u'w'})_0}, \tag{1}$$

$$T_* = \frac{-(\overline{w'\theta'})_0}{u_*}. \tag{2}$$

The characteristic length scale for surface layer turbulence is z, and the characteristic velocity and temperature scales are the shear-induced scales u_* and T_*, which tend to dominate in the region $z < -L$, where the Monin–Obukhov length L is

$$L = \frac{-u_*^3 T_0}{kg(\overline{w'\theta'_v})_0}. \tag{3}$$

Note that, whereas the ordinary temperature flux $\overline{w'\theta'}$ enters the definition of T_* [Eq. (2)], the flux of virtual potential temperature $\overline{w'\theta'_v}$ is used in the definition of L [Eq. (3)].

According to MO theory, then, if a turbulence moment is scaled with appropriate combinations of u_*, T_*, and z, in the surface layer, the nondimensional moment must 1) be an order 1 quantity (i.e., the moment must be normalized by MO scales), and 2) it must be a universal function of the ''stability parameter'' z/L. As was discussed in Johansson et al. (2001), the physical implication of MO similarity theory (if correct) is that the structure of the surface layer is determined by turbulence dynamics local to the surface, and results from shear-induced turbulent motions.

It would be surprising if the rather sweeping MO assumptions were to apply at all levels of detail to all turbulence moments. However, it might not be unreasonable to expect some level of correspondence in the surface layer. The value of exploring the validity and boundaries of the MO theory is both to improve our understanding of physical influences that organize boundary layer structure, and to develop useful approximation tools for application in prediction methodologies.

AH02 point out that a problem in MO theory is an insufficient number of independent variables. Because the theory assumes that only the surface shear velocity scale u_* characterizes surface layer turbulence structure, u_* must appear in both the length scale L and in the temperature scale T_*. Therefore, if a turbulence property in the surface layer is scaled with u_* and plotted against the stability parameter z/L, some level of correlation will necessarily result, complicating attempts to show conclusively with measurements the validity of MO theory in specific cases.

However, the existence of u_* in both the MO-scaled

Corresponding author address: Dr. Ulf Högström, Department of Earth Sciences, Meteorology, University of Uppsala, Villavägen 16, Uppsala S-75236, Sweden.
E-mail: ulf.hogstrom@met.uu.se

© 2002 American Meteorological Society

variable and in z/L does not imply perfect correlation, as is obvious when purposefully randomized data is tested (AH02). More importantly, the first requirement of similarity theory—that the physically correct scales should normalize the appropriate moment (making it order 1) over the parameter range in which the theory is supposed to be valid—does *not* follow from the existence of u_* in both the dependent- and independent-scaled variables. Thus, for example, the statement by AH02 in the paragraph after Eq. (11) that, ''Johansson et al. (2001) interpret these plots (Figs. 9 and 12) as demonstrating that w_* is the appropriate scaling variable for σ_h over most of the z_i/L range; but clearly the built-in correlation could weigh heavily in this conclusion,'' is not correct. The second half of the statement, ''clearly the built-in correlation could weigh heavily in this conclusion,'' does not follow from the first half, ''that w_* is the appropriate scaling,'' and vice versa. What should be questioned is the level of scatter about the perceived correlations that enters through the existence of u_* on both sides of the relationship and its cause.

2. Scatter in plots of ϕ_m and ϕ_h

AH02 question the Johansson et al. (2001) claim that larger scatter encountered in the plot of the normalized wind gradient ϕ_m (Figs. 1 and 6 of Johansson et al. 2001) against z/L, compared to the corresponding plot for the nondimensional temperature gradient ϕ_h (Figs. 2 and 16 of Johansson et al. 2001) is caused by influence of the boundary layer height z_i, where

$$\phi_m = \frac{kz}{u_*}\frac{\partial U}{\partial z}, \tag{4}$$

$$\phi_h = \frac{kz}{T_*}\frac{\partial \Theta}{\partial z}. \tag{5}$$

According to AH02, the larger scatter found in the conventional plot of ϕ_m compared to ϕ_h should be a result of variability in u_*, affecting ϕ_m more strongly than ϕ_h. In addition, ϕ_h may also contain a spurious correlation between $\overline{(w'\theta'_v)_0}$ in L, and $\overline{(w'\theta')_0}$ in T_*. The uncertainties in u_* combined with the spurious correlation in u_* should then give a larger contribution to the scatter in the plot of ϕ_m compared to that of ϕ_h.

AH02 show in their Fig. 1 the effect of a $\pm 10\%$ error in u_* on ϕ_m and ϕ_h, moving ϕ_m normal to the curve and ϕ_h along the fitted curve. This is in principal true, but it is too oversimplified to describe real data and thus, too simplified to draw conclusions from about the scatter in ϕ_m and ϕ_h, as AH02 do. AH02 assume, in their argument, that a measured error exists in the measured u_* but *not* in the measured temperature flux $\overline{(w'\theta')_0}$ (included in ϕ_h), which is highly unlikely. By also introducing a $\pm 10\%$ error in the temperature flux the result is much more complex, especially for ϕ_h, as shown in Fig. 1. Figure 1a shows that if the temperature flux also is altered, the displacement of ϕ_m is slightly reduced, since the variation in z/L becomes less, whereas ϕ_m stays the same. Figure 1b shows the effect on ϕ_h when the temperature flux is altered. In this case, not only z/L is effected but also the value of ϕ_h and thus the displacement pattern is much more complex compared to ϕ_m. With this more complex pattern, the scatter in ϕ_h is surprisingly low compared to ϕ_m.

The scatter in ϕ_m and ϕ_h can also be investigated from real measurements. According to MO theory the wind gradient shall be normalized with u_* and the temperature gradient with T_*, and hence these are the relevant parameters to investigate for scatter. If the larger scatter found in ϕ_m is related to measuring errors in u_*, it would be reflected as larger scatter in a $(1/u_*, z/L)$ plot compared to a $(1/T_*, z/L)$ plot, where the variable z/L is used instead of $1/u_*^3$, because it appears in both plots. As can be seen in Figs. 2a and 2b, the scatter in the variables is almost the same. It therefore seems unlikely that this alone is the source of the scatter.

Furthermore, note that wind gradient varies by a factor of 4 ($0.05\ s^{-1}$ to $0.2\ s^{-1}$) and the temperature gradient by a factor of 3 ($-0.01°C\ m^{-1}$ to $-0.03°C\ m^{-1}$), roughly the same range. In contrast, the range of variation in $1/T_*$ is a factor of 10 as compared to a factor of only 3 for $1/u_*$. This large difference in range implies that ϕ_h variations are dominated by variations in T_*, whereas the corresponding variations in ϕ_m are dependent more on variation in wind gradient. In addition, because $\phi_m \propto 1/u_*$ and $\phi_h \propto u_*$ while $z/L \propto u_*^{-3}$, variability in u_* is much more likely to create variability in the stability parameter z/L than in ϕ_m and ϕ_h (see, e.g., Figs. 1a and 1b).

Our argument that the larger variability observed in ϕ_m as compared with ϕ_h is a consequence of the boundary layer height can be further tested with earlier data of Högström (1974) collected at the same site. For logistical reasons, the vast majority of the data were collected during summer afternoon periods when the convective boundary layer is well developed and variability in z_i is not very large, strongly limiting the variation in z_i/L. As can be seen in Fig. 3, the scatter is very much less than in the corresponding Figs. 6 and 7 in Johansson et al. (2001). A direct result from the argument in Johansson et al. (2001) is that smaller scatter in ϕ_m is expected if the value of z_i/L is contained within a narrow range of values. This argument is therefore supported also by the data of Högström (1974).

The results for ϕ_m from Högström (1974) are also in good agreement with results from the Kansas experiment. In Businger et al. (1971), the scatter in their plot of ϕ_m (their Fig. 1) is not larger than the scatter in their plot of ϕ_h (their Fig. 2). Discussions with participants in the Kansas experiment indicate that those measurements were subject to similar logistical restrictions as were the Högström (1974) measurements, resulting in a similar restriction in the range of z_i/L of their data.

Even if some increase in the scatter in ϕ_m, as compared with ϕ_h, could be explained by uncertainties in

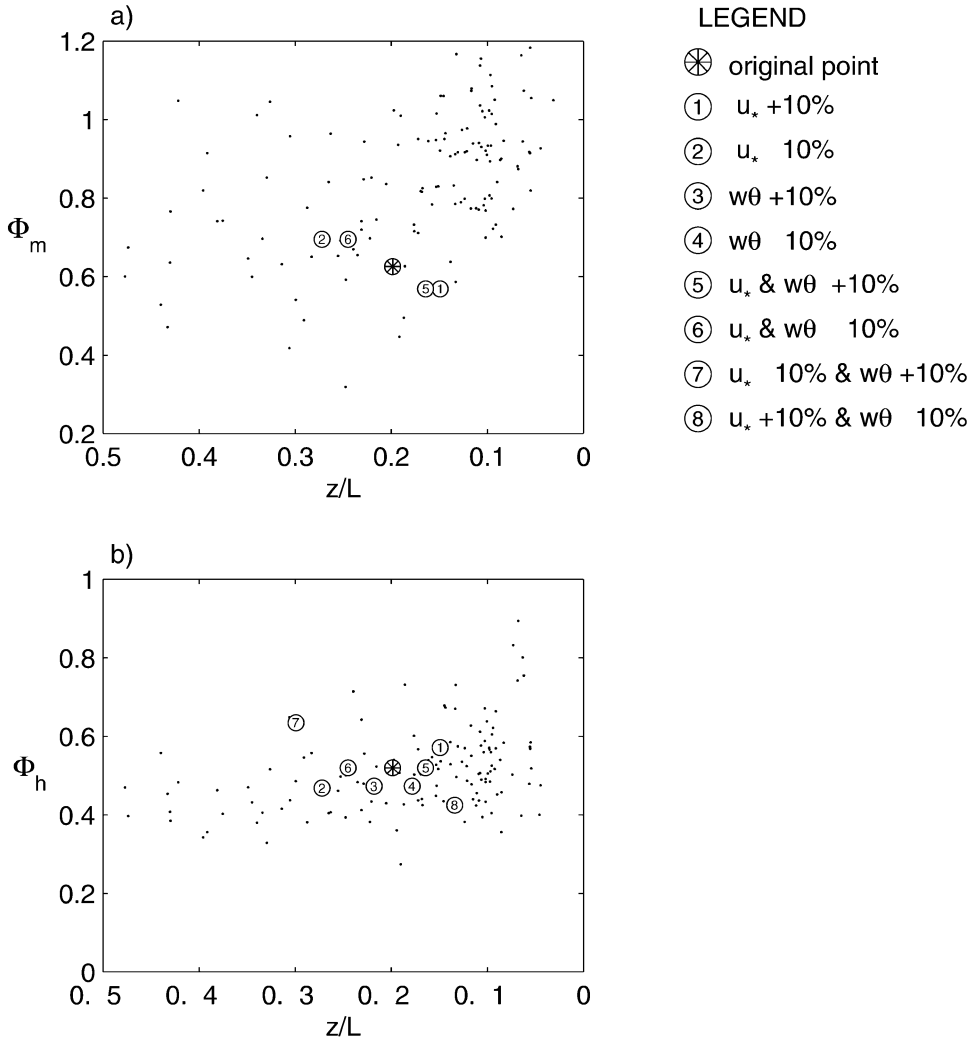

FIG. 1. Displacement of a measured point plotted against z/L when recalculated with u_* and $\overline{(w'\theta')_0}$ altered $\pm 10\%$ in different combinations (see legend). The small dots are measured values for comparison: (a) ϕ_m, (b) ϕ_h. Marker numbers 1 and 2 corresponds to the points in Fig. 1 in AH02.

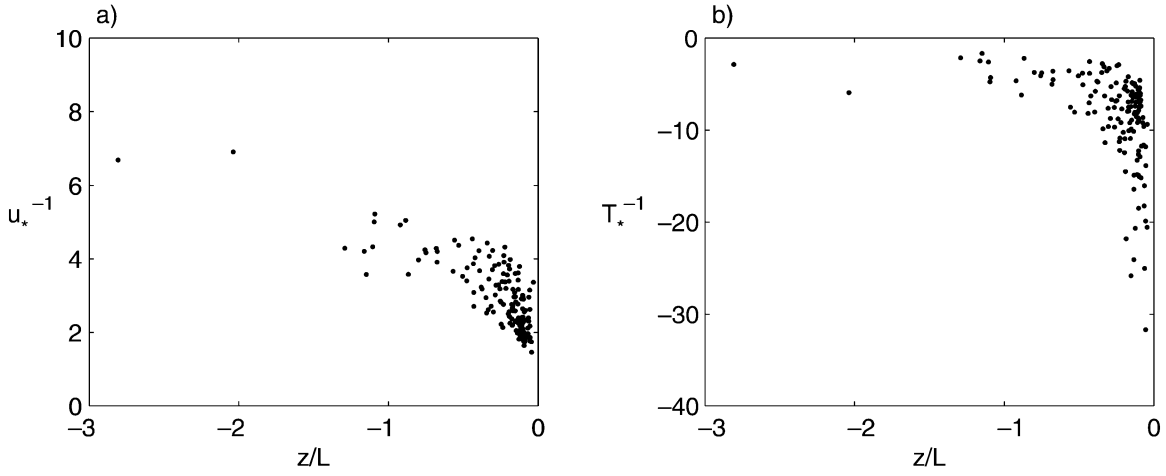

FIG. 2. (a) Plot of $1/u_*$ against z/L. (b) Plot of $1/T_*$ against z/L.

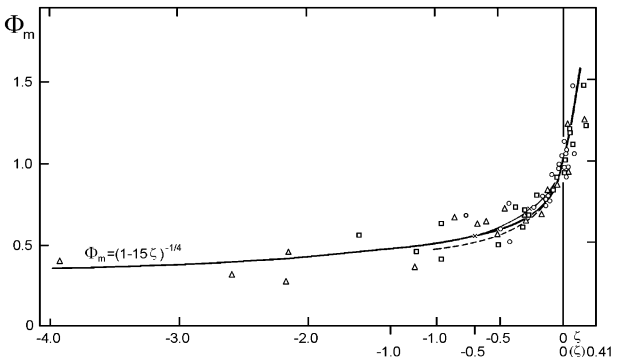

FIG. 3. Normalized wind gradient ϕ_m as a function of stability $\varsigma = z/L$ from an earlier experiment at the same site (Högström 1974).

u_* and/or spurious correlation as stated by AH02 they cannot explain the layering of ϕ_m with respect to z_i/L. To make this point in another way, consider the variation in normalized wind gradient with respect to the gradient Richardson number $\mathrm{Ri}_{\mathrm{grad}}$, rather than z/L, where

$$\mathrm{Ri}_{\mathrm{grad}} = \frac{g}{T_0}\frac{\dfrac{\partial \Theta}{\partial z}}{\left(\dfrac{\partial U}{\partial z}\right)^2}. \tag{6}$$

Plotted against $\mathrm{Ri}_{\mathrm{grad}}$, as opposed to z/L, the variables that experience spurious correlation will change and, more importantly, the relationship between z_i/L and z/L in the previous representation is removed. Figure 4a shows ϕ_m against z/L. As in Johansson et al. (2001), the data have been grouped with z_i/L according to $-5 < z_i/L < -0.5$, $-35 < z_i/L < -25$, and $z_i/L < -60$. In Fig. 4b, the same data for ϕ_m with the same z_i/L range have been replotted against $\mathrm{Ri}_{\mathrm{grad}}$. It is interesting to see that, while the scatter in ϕ_m decreases, the systematic layering of the data by z_i/L remains similar to Fig. 4a, and to the corresponding large eddy simulation (LES) results of Khanna and Brasseur (1997). It is very unlikely that ϕ_m plotted against two fundamentally different stability parameters, one that originates from fluxes (z/L) and one from gradients ($\mathrm{Ri}_{\mathrm{grad}}$), would display a similar behavior with respect to z_i/L, if the influence of z_i/L were not real. This demonstrates, as concluded by Johansson et al. (2001) and Khanna and Brasseur (1997), an influence of outer-scale ABL eddies on mean-flow structure in the surface layer.

3. Normalizing horizontal velocity variance

AH02 worry that the relation for $(\sigma_h/w_*)^2$ given in Johansson et al. [2001; see Eq. (7) below] suffers from spurious correlation, and hence that the conclusion that w_* is the characteristic velocity that normalizes σ_h over most of the z_i/L range might be incorrect. AH02 take particular issue with the empirical relationship

$$\left(\frac{\sigma_h}{w_*}\right)^2 = k^{2/3}\left(\frac{10}{-z_i/L} + 0.88\right)^{2/3}, \tag{7}$$

which was derived as a variation to Panofsky et al. (1977) to better fit the latest data, and written in a form that displays explicitly the normalization of σ_h. We pointed out above that the issue of spurious correlation between $(\sigma_h/w_*)^2$ and z_i/L and the requirement that $(\sigma_h/w_*)^2$ be an order 1 quantity are unrelated. Comparison of Figs. 8 and 9 in Johansson et al. (2001) shows that w_* is the appropriate scaling variable that normalizes σ_h in the surface layer.

According to Hicks (1981) there are two methods that can be used to test potentially spurious correlation: first by ''randomizing critical parts of the original data set,'' and second by ''producing a surrogate data set from ran-

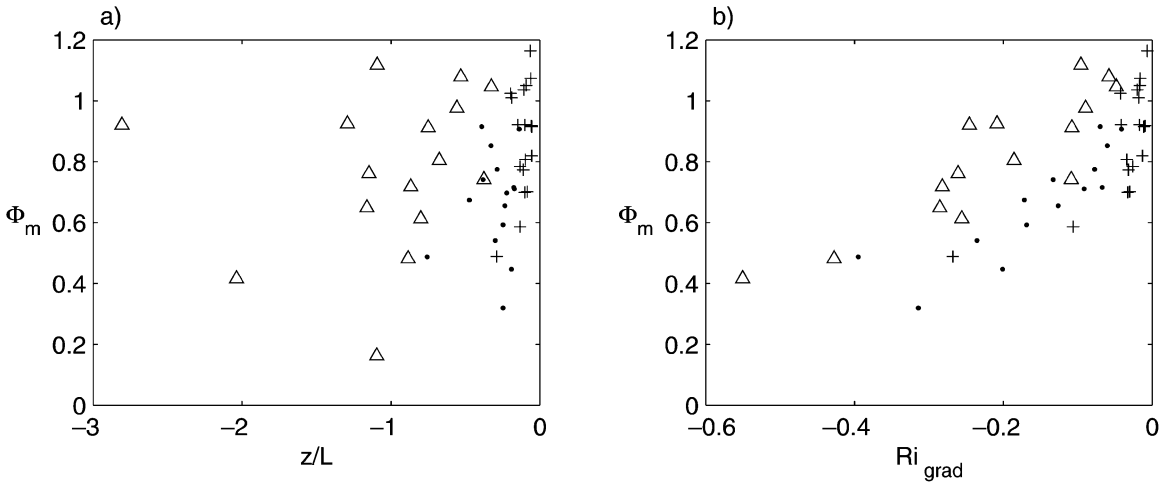

FIG. 4. (a) The normalized wind gradient plotted against the stability parameter z/L for measurements within the three z_i/L groups: pluses are $-5 < z_i/L < -0.5$, filled circles are $-35 < z_i/L < -25$, and triangles are $z_i/L < -60$. (b) Normalized wind gradient plotted against gradient Richardson number [Eq. (6)]. Symbols as in (a).

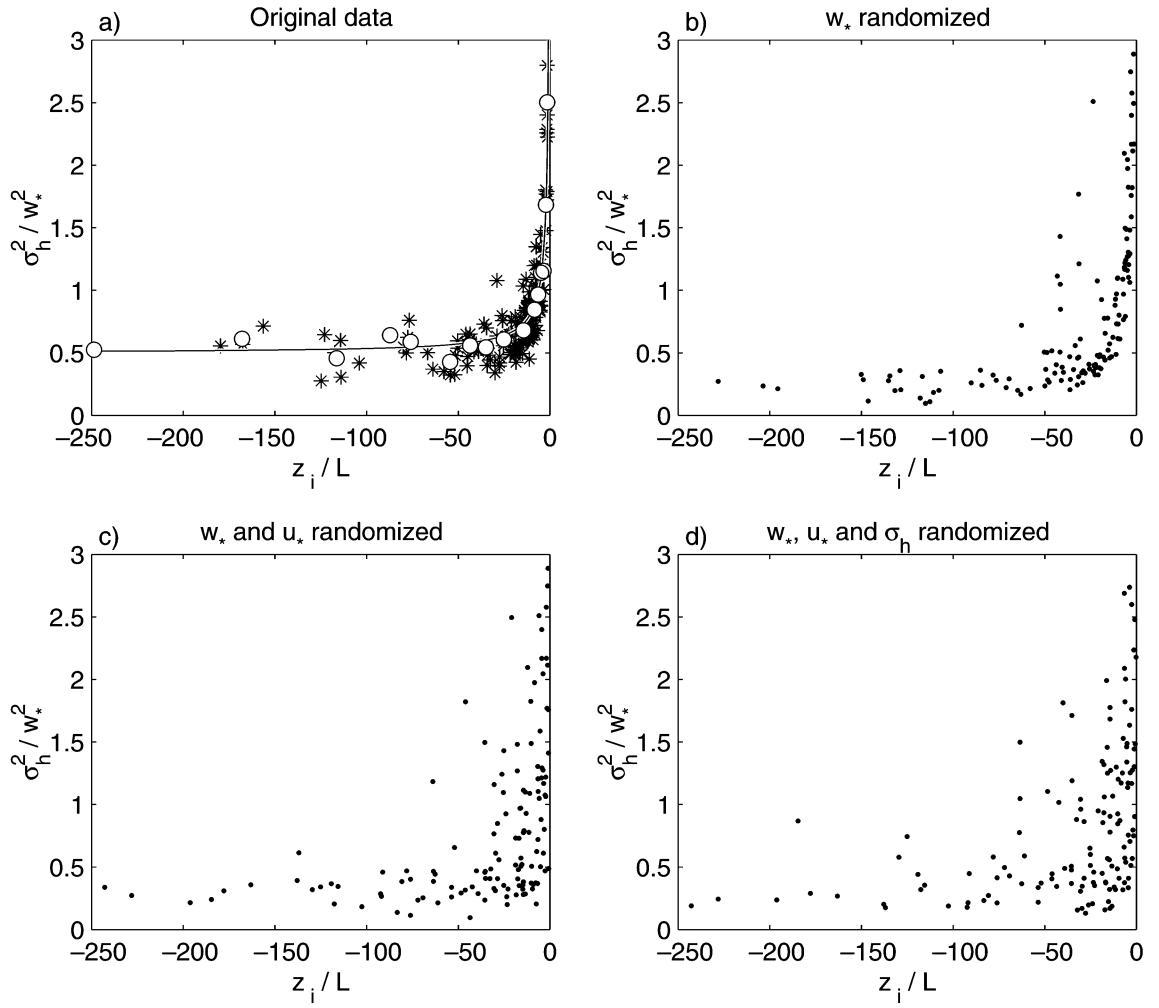

FIG. 5. (a) Horizontal velocity variance normalized by w_*^2 plotted against z_i/L. Stars are individual measurements; open circles are mean values over finite z_i/L ranges. The thin curve is Eq. (7) from Johansson et al. (2001). (b) Same as in (a), but with randomized values of w_* used in the calculation of z_i/L [Eq. (8)] and in $(\sigma_h/w_*)^2$. (c) Same as (b), but with randomized values for w_* and u_*. (d) Same as (b), but with randomized values for w_*, u_*, and σ_h.

dom numbers.'' In the absence of access to our data, AH02 applied the second approach. However, in doing so, they removed some of the randomness in their sample by discarding random values for $(\sigma_h/w_*)^2$ outside the range 0.2 to 6 (while z_i/L was allowed to vary between -0.5 and -200). In effect, then, AH02 have demanded that their ''random'' $(\sigma_h/w_*)^2$ values be order 1 and therefore that w_* normalize σ_h while allowing z_i/L to vary over 2 to 3 orders of magnitude. They discovered that a plot of their partially randomized $(\sigma_h/w_*)^2$ versus z_i/L has the general trends of Fig. 5a (taken from Johansson et al. 2001), but with significantly greater scatter. Had AH02 allowed $(\sigma_h/w_*)^2$ to vary over 2 to 3 orders of magnitude like z_i/L, there would be an even greater difference in scatter than what is currently apparent between their Fig. 2 and Fig. 5a below. More importantly, they would have demonstrated further that w_* is the appropriate scaling variable for σ_h in that it both nondimensionalizes and normalizes σ_h.

AH02 argue that the best way to see whether a useful correlation has been found between $(\sigma_h/w_*)^2$ and z_i/L (Fig. 5a) is to investigate the level of spurious correlation by randomizing w_* and then recalculating z_i/L from

$$\frac{z_i}{L} = -\frac{w_*^3}{u_*^3}k, \tag{8}$$

from which randomized $(\sigma_h/w_*)^2$ is to be plotted against recalculated z_i/L. In the words of AH02, if then the resulting plot would look ''unpublishably confusing,'' the result would be that w_* is indeed a useful nondimensionalization variable. In the above proposition by AH02, ''w_* is chosen as the 'critical' variable in this expression.'' As discussed above, however, the ''use-

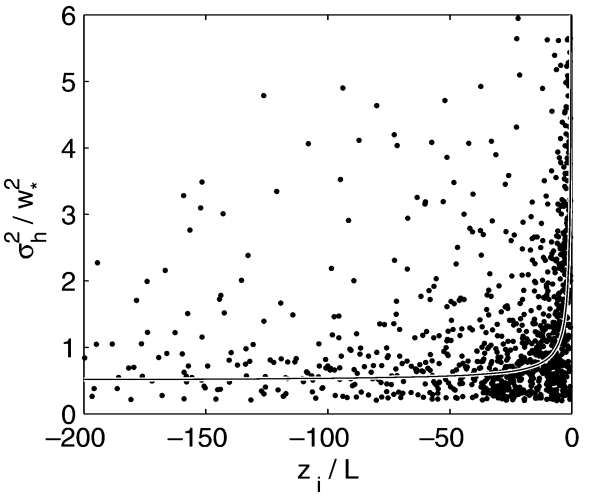

FIG. 6. Plot of $(\sigma_h/w_*)^2$ against z_i/L for a partially randomized dataset containing 1019 points. The following variables have been randomly generated: σ_h, u_*, and w_*. The values of z_i/L have been calculated from Eq. (8). The thin curve is Eq. (7).

fulness'' of w_* as a nondimensionalization variable is first that it normalizes σ_h^2 when $z_i/L < -1$, an issue unrelated to the spurious correlation effect pointed out by AH02.

Following the suggestion of AH02, our measured set of w_* has been randomized and used to construct Fig. 5b. By comparing the plot with the original figure from Johansson et al.'s (2001) Fig. 5a, we see that although there is more scatter, there is still a resemblance in the shape between the two figures, a reflection of the artificial correlation pointed out by AH02. However, the values of $(\sigma_h/w_*)^2$ are generally lower compared to the original data in Fig. 5a for $z_i/L < -1$, a reflection of the appropriateness of w_* as the appropriate characteristic velocity scale that normalizes σ_h. However, in Fig. 5b we have kept the original physically meaningful connection between the other variables u_* and σ_h. If these variables are also randomized, a gradual disappearance of the pattern that exist in Figs. 5a and 5b can be seen in Figs. 5c–d. It is interesting to compare Fig. 5d with Fig. 2 from AH02. Both figures have similarly randomized data, but the figure by AH02 still shows a pattern that can be interpreted to follow roughly the expression for $(\sigma_h/w_*)^2$ [Eq. (7)]. AH02 interpreted this rough correspondence to conclude that randomized data more-or-less automatically follows Eq. (7) (the line in their Fig. 2), as a reflection of the spurious correlation. However, their data were only partially randomized. As can be seen in Fig. 5d, by using real data that has been fully randomized (see description above) the pattern more-or-less disappears.

To see whether the size of the random dataset that AH02 draw their conclusions from is important, a larger random dataset was constructed, using the same criteria as AH02 on σ_h, u_*, and w_*. Our partially randomized dataset contains 1019 points. The result is shown in Fig. 6. As can be seen in the figure, there is a tendency for the data to cluster around the curve [Eq. (7)], caused by the common variable w_*, but the scatter is much larger compared to the scatter of the measurements in Fig. 5a. By calculating the residual variance [Eq. (9)] for the curve [Eq. (7)] and the partially randomized dataset in Fig. 6, a measure of the scatter in the figure is

$$S_q^2 = \frac{\sum_{i=1}^{n} (d_{i\min})^2}{n - 2}, \tag{9}$$

where $d_{\min}$ represents the shortest distance from a point $[z_i/L, (\sigma_h/w_*)^2]$ to the curve [Eq. (7)]. The residual variance for the partially randomized data in Fig. 6 is 1.12, which shall be compared to the value 0.03, which is the residual value for the measurements in Fig. 5a. This shows that Eq. (7) is a *very* good fit to the measurements but not to the partially randomized dataset. The residual variance calculated from Fig. 2 in AH02 is 0.77, which is slightly lower then 1.12 but still much larger than 0.03 obtained for the measurements in Fig. 5a. We argue that the constraints that AH02 placed on their partially randomized $(\sigma_h/w_*)^2$ and the low amount of points in their random dataset leads to a curve that is of the form $(\sigma_h/w_*)^2 \sim O(1)$ in the range $-100 < z_i/L < -20$, thus giving a misleading result.

From these considerations we argue that Fig. 5d can be called ''unpublishably confusing,'' that the parameter w_* is the relevant scaling parameter for the horizontal velocity variance, and that the relation for $(\sigma_h/w_*)^2$ given in Johansson et al. (2001) [Eq. (7)] can be considered useful. In view of Fig. 5d, it is evident that much of the measured relationship between $(\sigma_h/w_*)^2$ and z_i/L in Fig. 5a results from physically meaningful connections between them.

Toward the end of their discussion on horizontal velocity variance, AH02 show that Eq. (8) can be used to rewrite Eq. (7) as

$$\sigma_h^2 = [10u_*^3 + 0.88kw_*^3]^{2/3}. \tag{10}$$

This relation is completely equivalent to Eq. (7), but the two equations emphasize different features and are therefore both useful, especially when interpreted together. The form Eq. (7) shows explicitly the influence of boundary layer depth through z_i/L on horizontal velocity variance, the primary theme in Johansson et al. (2001). We conclude that the z_i-scale motions in the ABL influence certain aspects of turbulence structure near the ground, and that this influence increases as buoyancy production of large-scale atmospheric turbulence increases relative to shear generation near the surface. This is a useful conclusion with clear physical interpretation. AH02 point out that Eq. (10) allows for a related interpretation, that ''what causes the variability in the horizontal wind components [is] shear driven turbulence in high winds and convectively driven turbulence in low winds.'' This too is a valuable insight,

which, when combined with that just above, leads one to conclude that as buoyancy production increases relative to shear production (decreasing $z_i/L < -1$), the relative contribution of shear to the variability of horizontal velocity fluctuations decreases [Eq. (10)], and that the primary source of the shear contribution to horizontal velocity variance in the surface layer is the sweeping effect of the z_i-scale eddies near the ground.

Consider the behavior of the horizontal velocity variance in the limits of neutrality and free convection. In the neutral limit ($w_* \to 0$), Eq. (10) becomes

$$\sigma_h^2 \to 4.6u_*^2. \tag{11}$$

AH02's Eq. (10) is, in terms of the variance of the lateral component σ_v^2, giving the constant of proportionality as 3.6. Considering $\sigma_h^2 = 1/2(\sigma_u^2 + \sigma_v^2)$ and $\sigma_u^2 > \sigma_v^2$, our value of 4.6 must be said to be in good agreement with AH02's result. In the free convection limit ($u_* \to 0$), Eq. (10) becomes

$$\sigma_h^2 \to 0.92kw_*^2. \tag{12}$$

Taking the von Kármán constant k to be 0.4, the constant of proportionality is 0.50, which should be compared with AH02's value 0.35. Given the systematic difference between σ_h^2 and σ_v^2 discussed above, this must also be considered as reasonably close to our value. We conclude that the expression given in Johansson et al. (2001) for σ_h^2 [Eq. (7)] provides a good overall description from neutral to free convection, and that both forms Eqs. (7) and (10) are useful for interpretation.

The final remark by AH02, that it is useless to even try to present general expressions for the variance of the horizontal wind because of the influence of a multitude of mesoscale motions is far too defeatist in our view. It is true that different studies report a range of values for the numerical factor in the neutral and free convection limit, Eqs. (11) and (12), respectively; but this is to a large extent a result of the employment of different effective low-frequency cutoff frequencies in the different studies. In fact, the reasonable agreement demonstrated above between our results and the corresponding results from AH02's Eq. (10) in the limits of neutrality and free convection is a good demonstration that the general statement of AH02 concerning the possibility to quantify the variance of the horizontal wind is far too pessimistic.

4. Concluding remarks

To conclude, we insist that the reason for the larger scatter in ϕ_m compared to ϕ_h is the influence of the boundary layer height, and that the variable z_i/L can be used to show this. Concerning the expression for the horizontal wind variance [Eq. (7)], the relationship is based on physical grounds and not on spurious correlation, and thus w_* is the appropriate scaling variable over most z_i/L ranges as stated in Johansson et al. (2001) and in Khanna and Brasseur (1997).

REFERENCES

Andreas, E. L, and B. B. Hicks, 2002: Comments on ''Critical test of the validity of Monin–Obukhov similarity during convective conditions.'' *J. Atmos. Sci.,* **59,** 2605–2607.

Businger, J. A., J. C. Wyngaard, Y. Izumi, and E. F. Bradley, 1971: Flux-profile relationships in the atmospheric surface layer. *J. Atmos. Sci.,* **28,** 181–189.

Hicks, B. B., 1981: An examination of turbulence statistics in the surface layer. *Bound.-Layer Meteor.,* **21,** 398–402.

Högström, U., 1974: A field study of the turbulent fluxes of heat, water vapour and momentum at a ''typical'' agricultural site. *Quart. J. Roy. Meteor. Soc.,* **100,** 624–639.

Johansson, C., A. Smedman, U. Högström, J. G. Brasseur, and S. Khanna, 2001: Critical test of the validity of Monin–Obukhov similarity during convective conditions. *J. Atmos. Sci.,* **58,** 1549–1566.

Khanna, S., and J. G. Brasseur, 1997: Analysis of Monin–Obukhov similarity theory from large-eddy simulation. *J. Fluid Mech.,* **345,** 251–286.

Panofsky, H. A., H. Tennekes, D. H. Lenschow, and J. C. Wyngaard, 1977: The characteristics of turbulent velocity components in the surface layer under convective conditions. *Bound.-Layer Meteor.,* **11,** 355–361.